Table of Contents for the Supplemental material

Supplementary Figure 1. Doxycycline alone does not alter transepithelial resistance and claudin-8 expression.

Supplementary Figure 2. ENaC γ-subunit silencing decreases claudin-8 expression in cultured collecting duct principal cells.

Supplementary Figure 3. Effect of ENaC α-subunit silencing on claudin-8 abundance in cultured collecting duct principal cells.

Supplementary Figure 4. Effect of ENaC β-subunit silencing on claudin-8 abundance in cultured collecting duct principal cells.

Supplementary Figure 5. Cell-surface protein biotinylation from cells overexpressing and silencing claudin-8 and cells overexpressing claudin-2 and claudin-10.

Supplementary Figure 6. Effect of sodium and chloride transport on measured transepithelial potential difference.

Supplementary Figure 7. Effect of nephron-specific α-ENaC and β-ENaC knockout on claudin-8 abundance.

Supplementary Figure 8. Speculated mechanism of interaction between ENaC γ-subunit and claudin-8.

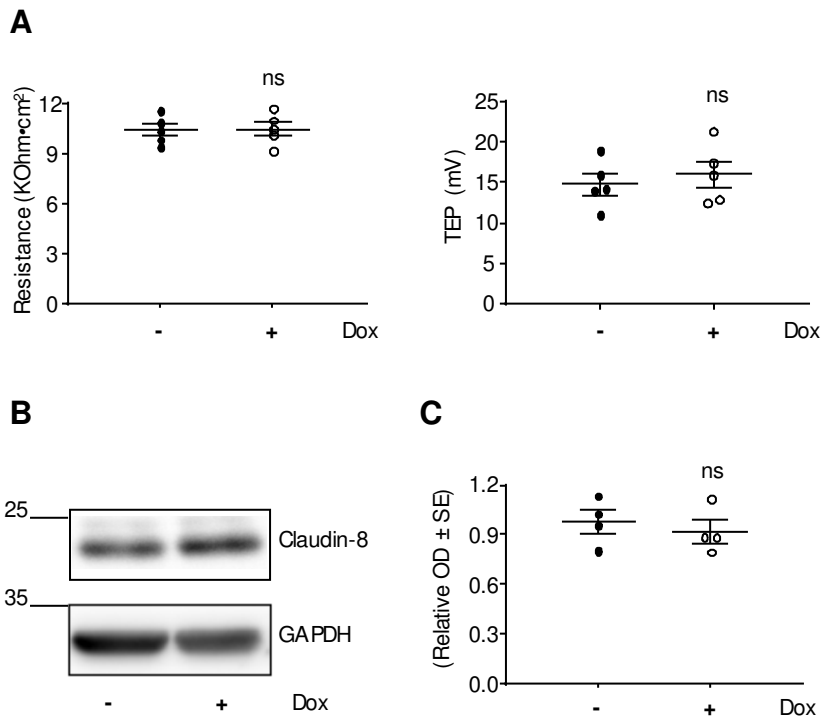

Supplementary Figure 1. Doxycycline alone does not alter transepithelial resistance, transepithelial potential and claudin-8 expression. A, Measured transepithelial resistance (R; left panel) and potential difference (TEP; right panel, lumen negative). B, Representative immunoblots showing the effect of Dox treatment on claudin-8 protein abundance. GAPDH was used as a loading control. C, Bar graphs depicting relative densitometric quantification of immunoblots from 4 independent experiments. Results are means ± SEM from 4 independent experiments. Statistical analysis was performed by Student's t-test.

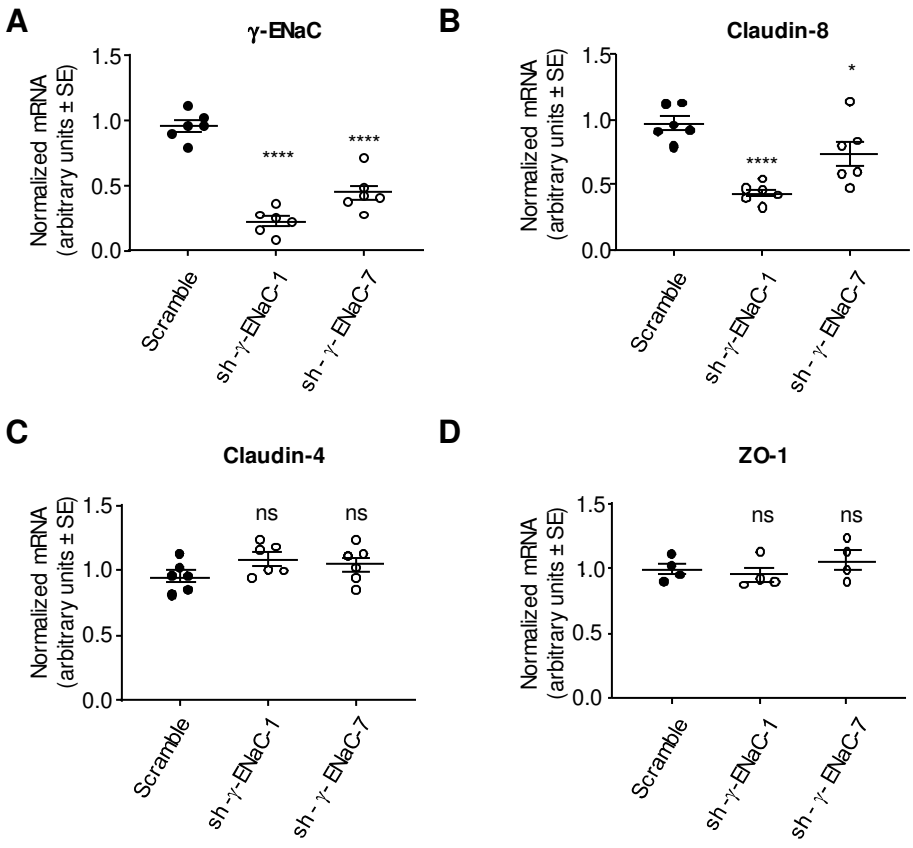

Supplementary Figure 2. ENaC γ-subunit silencing decreases claudin-8 expression in cultured collecting duct principal cells. $mCCD_{cl1}$ cells transduced with lentiviruses encoding either scramble shRNA (scramble) or shRNAs targeting mouse γ-ENaC (sh-γ-ENaC-1 and sh-γ-ENaC-7) were grown to confluence on filters. A-D, γ-ENaC, claudin-8, claudin-4 and ZO-1 mRNA levels were assessed by Real-Time PCR. Results are means ± SEM from 4 independent experiments. Statistical analysis was performed by one-way ANOVA; * $p < 0.05$; ** $p < 0.01$; *** $p < 0.001$.

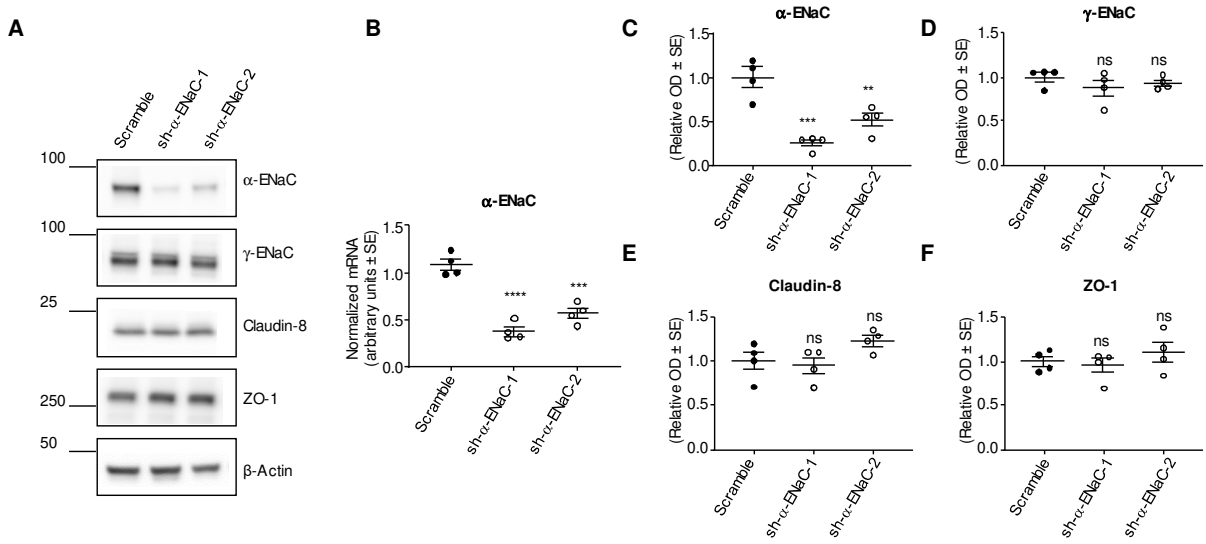

Supplementary Figure 3. Effect of α-ENaC silencing on claudin-8 abundance in cultured collecting duct principal cells. $mCCD_{cl1}$ cells transduced with lentiviruses encoding either scramble shRNA (scramble) or shRNAs targeting mouse α-ENaC (sh-α-ENaC-1 and sh-α-ENaC-2) were grown to confluence on filters. (A) Representative immunoblots showing the effect of α-ENaC silencing on α-ENaC, γ-ENaC, claudin-8 and ZO-1 protein levels. β-actin was used as the loading control. (B) α-ENaC mRNA levels assessed by Real-Time PCR. C-F relative densitometric quantification of immunoblots (shown in A) from 4 independent experiments. Statistical analysis was performed by one-way ANOVA; * $p < 0.05$; ** $p < 0.01$; *** $p < 0.001$.

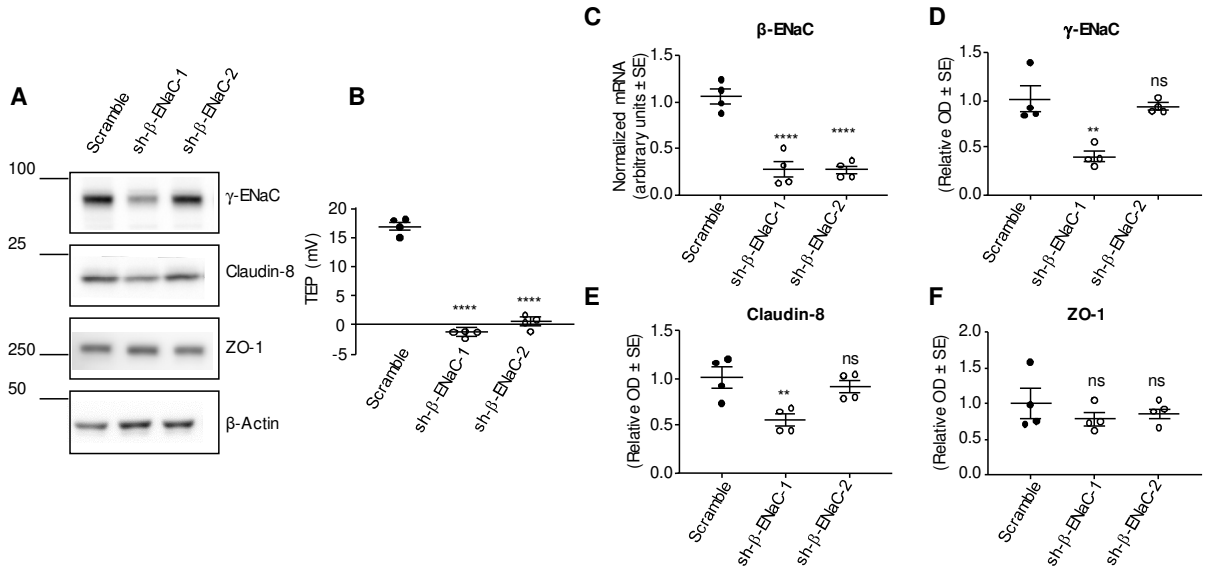

Supplementary Figure 4. Effect of β-ENaC silencing on claudin-8 abundance in cultured collecting duct principal cells. $mCCD_{cl1}$ cells transduced with lentiviruses encoding either scramble shRNA (scramble) or shRNAs targeting mouse β-ENaC (sh-β-ENaC-1 and sh-β-ENaC-2) were grown to confluence on filters. (A) Representative immunoblots showing the effect of β-ENaC silencing on γ-ENaC, claudin-8 and ZO-1 protein levels. β-actin was used as the loading control. Measured transepithelial potential difference (TEP, lumen negative) (B) and β-ENaC mRNA levels assessed by Real-Time PCR (C) were used to validate ENaC β-subunit silencing efficacy since we cannot obtain a satisfying signal to noise ratio with the antibody against β-ENaC in mCCD cells. D-F relative densitometric quantification of immunoblots (shown in A) from 4 independent experiments. Statistical analysis was performed by one-way ANOVA; * $p < 0.05$; ** $p < 0.01$; *** $p < 0.001$.

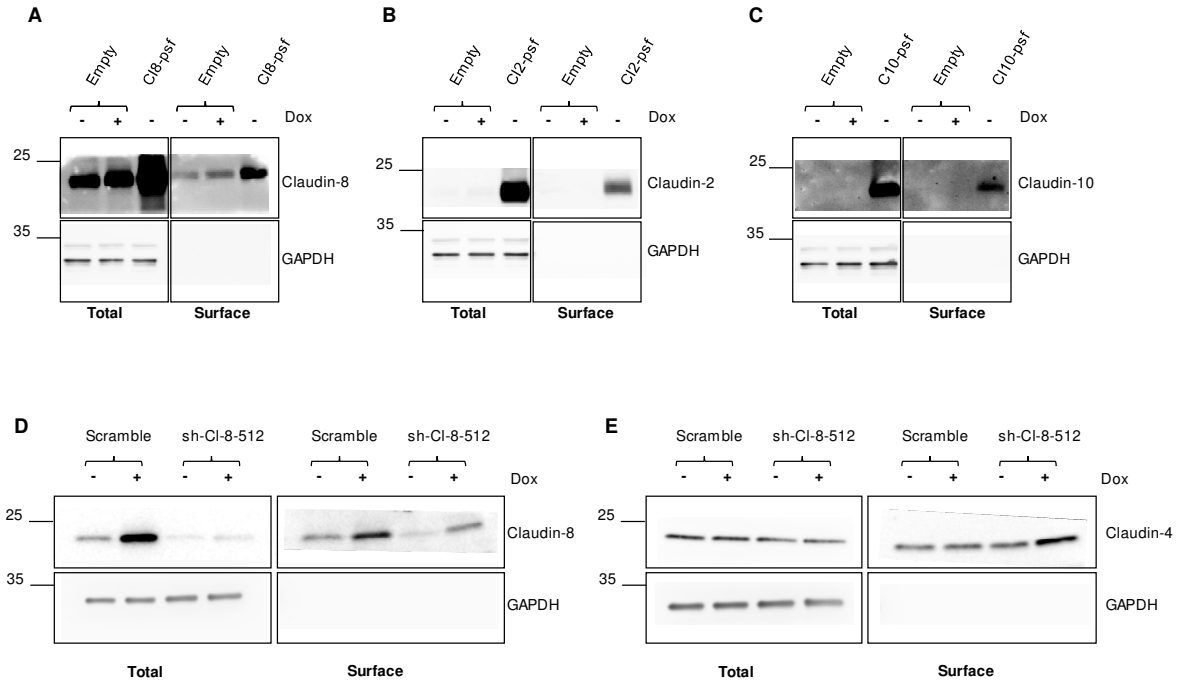

Supplementary Figure 5. Cell-surface protein biotinylation from cells overexpressing and silencing claudin-8 and cells overexpressing claudin-2 and claudin-10. γ-ENaC-TetOn- mCCD cells were first transduced with empty lentiviruses (empty) or that encoding wild-type mouse claudin-8 (Cl8-psf), claudin-2 (Cl2-psf) or claudin-10 (Cl10-psf). For the silencing of claudin-8, cells were transduced with lentiviruses encoding either scramble shRNA (scramble) or shRNA targeting mouse claudin-8 (shCl-8-512). Transduced cells were grown to confluence on filters and treated or not with 1.25 µg/ml doxycycline (Dox) for 2.5 days. Aliquots of total cell extract and biotinylated proteins were analyzed by western blotting. Cell surface and total expression levels of claudin-8 are shown in (A and D), claudin-2 in (B), claudin-10 in (C) and claudin-4 (E).

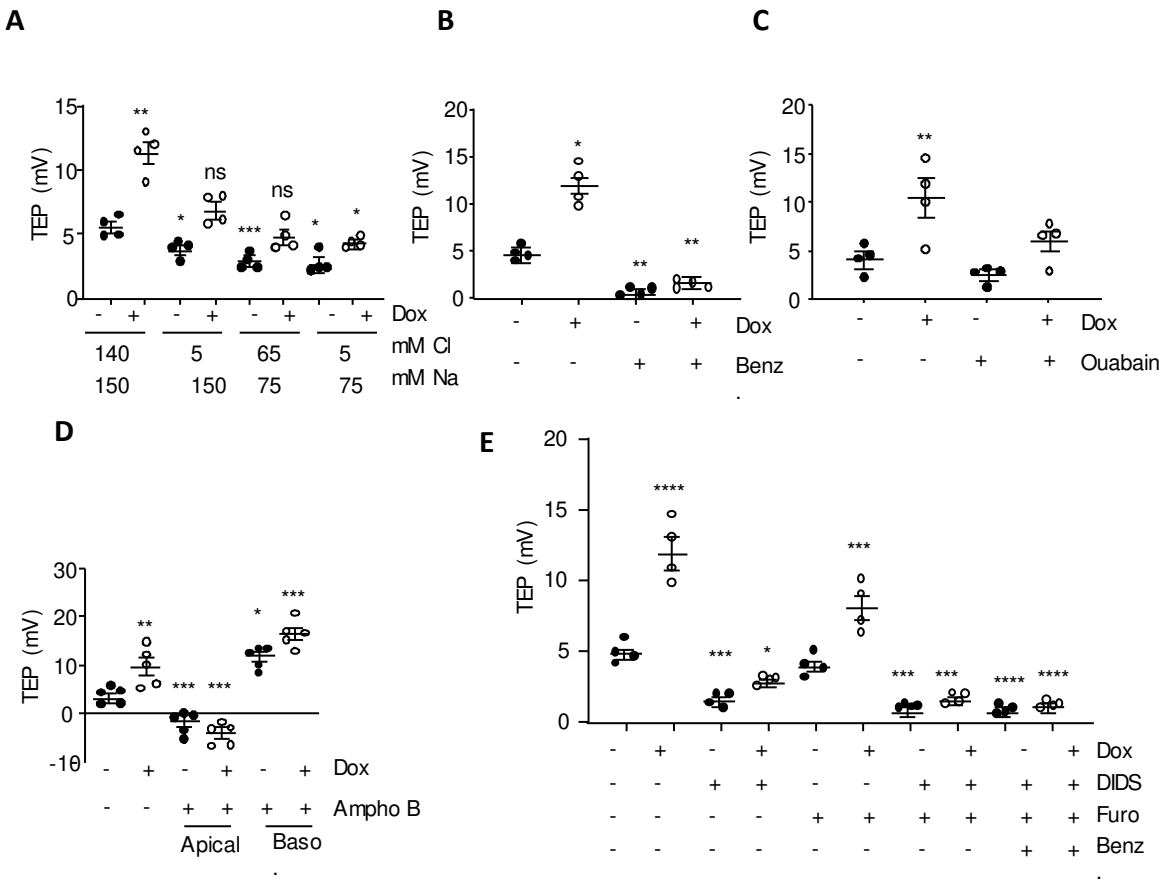

Supplementary Figure 6. Effect of sodium and chloride transport on measured transepithelial potential difference. γ-ENaC-TetOn-mCCD cells were grown to confluence on filters and treated or not with 1.25 µg/ml doxycycline (Dox) for 2.5 days to induce ENaC γ-subunit overexpression. A-E, Apical medium was removed and replaced for 24 h by iso-osmotic medium containing different concentrations of NaCl, Na-Gluconate or Choline-Cl (A). Cells were treated for 24 h with 10 µM benzamil (B), 1 µM ouabain (C), 50 µg/ml amphotericin B (D) or chloride transport blockers (10 µM Furosemide and 100 µM DIDS) (E). Potential difference was measured using a Millicell-ERS volt-Ohm meter, lumen negative. Results are means ± SEM from 4 independent experiments. Statistical analysis was performed by one-way ANOVA ; * $p < 0.05$; ** $p < 0.01$; *** $p < 0.001$.

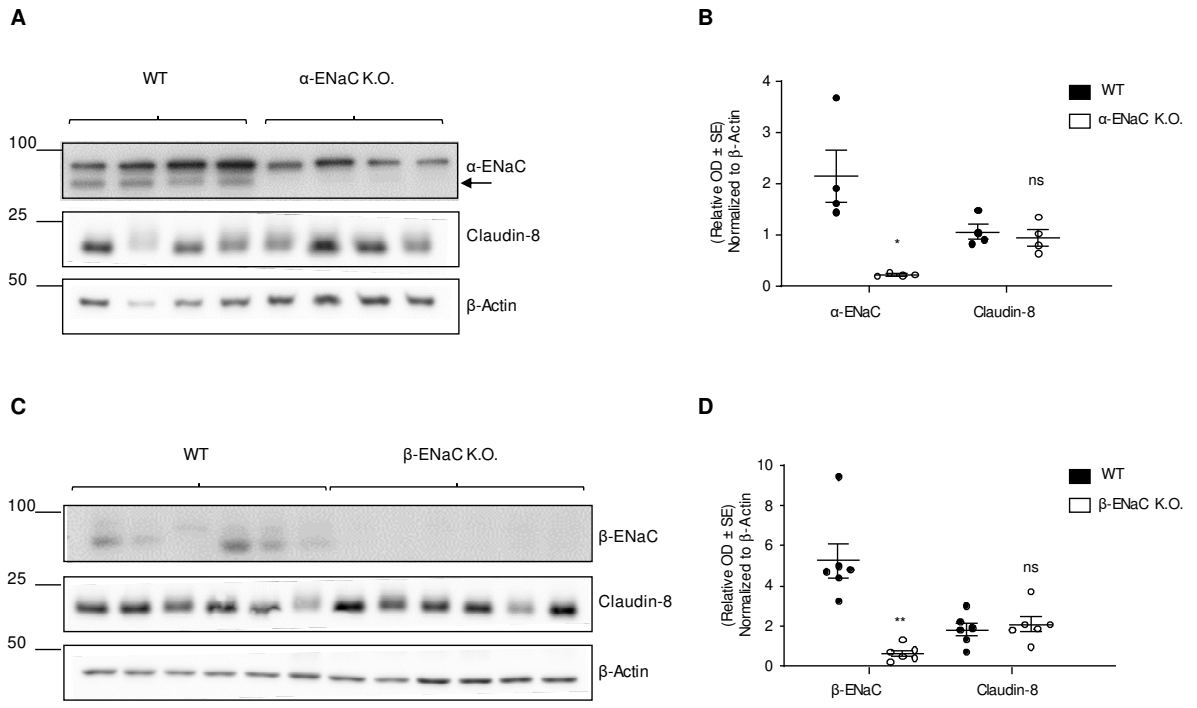

Supplementary Figure 7. Effect of nephron-specific α-ENaC and β-ENaC knockout on claudin-8 abundance. A, Representative immunoblots showing the effect of α-ENaC knockout on claudin-8 abundance in kidney cortex (controls, n = 4 and experimental α-ENaC KO mice: n = 4). B, quantification of protein expression levels normalized to β-actin protein expression levels (C) Representative immunoblots showing the effect of β-ENaC knockout on claudin-8 abundance in kidney cortex (controls, n = 6 and experimental β-ENaC KO mice: n = 6). (D) Quantification of protein expression levels normalized to β-actin protein expression levels. Results are presented as mean ± SEM. Statistical analysis was performed by Mann-Whitney U-test; * $p < 0.05$.

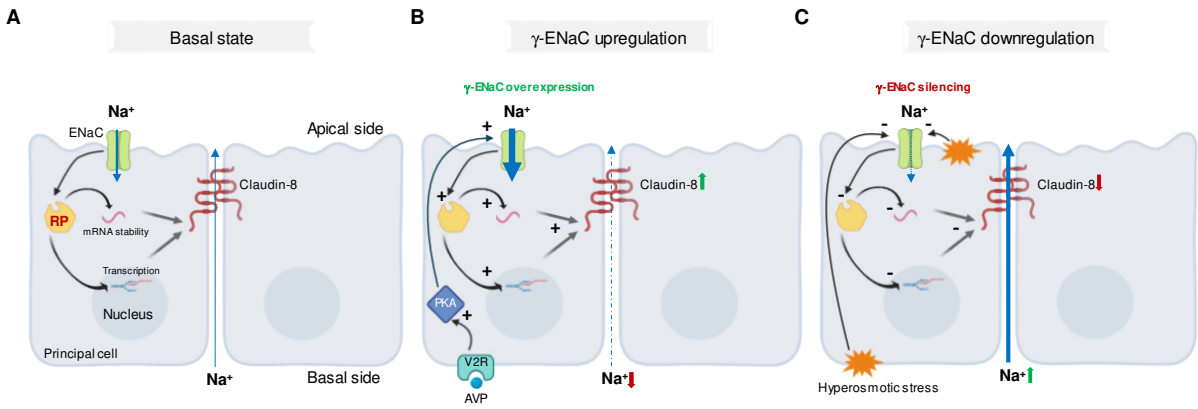

Supplementary Figure 8. Speculated mechanism of interaction between ENaC γ-subunit and claudin-8. The mechanism through which interaction between γ-ENaC subunit and claudin-8 takes place is still unclear. Herein, our results demonstrate that physiologic and genetic modulation of γ-ENaC affects claudin-8 abundance in mCCD cells and we confirmed this interaction *in vivo*. Our results are consistent with the hypothesis that γ-ENaC directly interacts with a regulatory protein (RP) which controls claudin-8 transcription and/or claudin-8 mRNA stability as shown in **A**. The stimulation of γ-ENaC by vasopressin (AVP) or its overexpression in mCCD cells, enhances the activity of the regulatory protein (RP) leading to more claudin-8 mRNA expression and higher claudin-8 protein abundance, resulting in a decreased sodium back-flux (**B**). Conversely, the downregulation of γ-ENaC for example by hyperosmotic stress (apical and basal sides) or its silencing in mCCD cells, reduces the activity of the regulatory protein (RP) and then claudin-8 abundance at the mRNA and the protein levels leading to an increased sodium back-flux (**C**).